

Short-term warming supports mineral-associated carbon accrual in abandoned croplands

Received: 18 June 2024

Accepted: 26 December 2024

Published online: 02 January 2025

 Check for updates

Zhenrui Zhang¹, Hui Gao¹, Xiaoxia Gao², Shurui Huang¹, Shuli Niu¹,
Emanuele Lugato¹ & Xinghui Xia¹

Effective soil organic carbon (SOC) management can mitigate the impact of climate warming. However, the response of different SOC fractions to warming in abandoned croplands remains unclear. Here, categorizing SOC into particulate and mineral-associated organic carbon (POC and MAOC) with physical fractionation, we investigate the responses of POC and MAOC content and temperature sensitivity (Q_{10}) to warming through a 3-year *in situ* warming experiment (+1.6 °C) in abandoned croplands across 12 sites in China (latitude: 22.33–46.58°N). Our results indicate that POC content remains unchanged while MAOC content significantly increases under warming. POC and MAOC content changes are mainly influenced by root biomass and microbial necromass carbon changes, respectively. The Q_{10} of MAOC is significantly lower than that of POC regardless of the warming or control treatment, suggesting that MAOC represents the most persistent and least vulnerable carbon fraction within SOC. Collectively, the sequestration of stable soil carbon can be enhanced in abandoned croplands under short-term warming.

Soil organic carbon (SOC) is the largest terrestrial carbon pool, 2 to 3 times greater than that of vegetation and the atmospheric carbon pool¹, consequently effective SOC management can mitigate the impact of climatic warming². Agricultural ecosystems cover approximately 38% of the global land area³, with cultivation leading to SOC losses driven by both soil disturbance⁴ and the increased microbial activity stimulated by warming⁵. It is estimated that global croplands lose between 0.3 to 1.0 Pg C year⁻¹ globally³. Meanwhile, due to unsatisfactory land suitability (such as declining soil fertility) and socio-economic drivers (such as urbanization or low cost-effectiveness of agricultural products), cropland abandonment is on the rise and expanding rapidly across various regions worldwide^{6,7}. Until now, abandoned cropland accounts for approximately 10% to 25% of global cropland area^{6,8}. Natural recovery process by secondary succession is generally beneficial for SOC accrual in abandoned croplands³, but the

impact of warming on SOC in this transitional ecosystem is not well understood. Furthermore, the transformation from conventional croplands to abandoned croplands and climate warming can change the traits of plants and microorganisms⁹, thereby altering the proportion of different SOC fractions.

Notably, SOC can be physically fractionated into particulate organic carbon (POC) and mineral-associated organic carbon (MAOC)¹⁰, as recently done in studies predominantly focused on POC and MAOC content in different ecosystems^{4,9,11}. In addition, due to the complexity and heterogeneity of POC and MAOC, the impact of climate warming on them may differ¹². POC is primarily considered to originate from plant fragmentation, while MAOC is formed through the sorption of low molecular weight organic carbon leached from plants or transformed by microorganisms to minerals¹³. In certain conditions, warming may enhance plant productivity, increasing the

¹Key Laboratory of Water and Sediment Sciences of Ministry of Education, State Key Laboratory of Water Environment Simulation, School of Environment, Beijing Normal University, Beijing, China. ²School of Ecology and Nature Conservation, Beijing Forestry University, Beijing, China. ³Key Laboratory of Ecosystem Network Observation and Modeling, Institute of Geographic Sciences and Natural Resources Research, Chinese Academy of Sciences, Beijing, China.

⁴European Commission, Joint Research Centre (JRC), Ispra, Italy.  e-mail: xiaxh@bnu.edu.cn

input of plant-derived carbon and thereby enhancing SOC content¹⁴. According to the “microbial efficiency-matrix stabilization” hypothesis¹⁵, when the input of plant-derived carbon is primarily composed of low molecular weight, labile and high-quality compounds, it promotes an increase in MAOC content. This is because such compounds are efficiently utilized by microorganisms and transformed into microbial necromass carbon (MNC) through the “microbial carbon pump”¹⁶, and then subsequently adsorbed by minerals to form MAOC¹⁷. Conversely, when the input of plant-derived carbon mainly consists of low-quality compounds, it favors an increase in POC content¹⁸. Abandoned croplands in China are undergoing natural recovery processes, which are dominated by grass species¹⁹. Plant-derived carbon from grass exhibits characteristics of low C/N and lignin/N ratios, enabling microorganisms to effectively convert it into MNC through the microbial carbon pump^{20,21}. However, whether increased input under warming conditions can enhance MAOC content in abandoned croplands, to date, has rarely been explicitly explored in any experimental studies.

Recently, researchers have increasingly paid attention to the temperature sensitivity (commonly represented by the Q_{10} , a constant for the change in SOC decomposition rate with a 10 °C increase in temperature) of different SOC fractions, given its pivotal role in predicting soil carbon dynamics²². However, our understanding is still constrained by two aspects. Firstly, previous studies on the Q_{10} of POC and MAOC have been largely confined to laboratory or single-site scales^{23,24}, lacking large-scale observational evidence. While these studies have contributed to understanding the Q_{10} of POC and MAOC, discrepancies in the classification of POC and MAOC and the methods used to determine their Q_{10} across different studies can lead to diverse results^{24,25}. Secondly, existing research on the Q_{10} of POC and MAOC primarily focused on comparing their Q_{10} values^{24,25}. In theory, POC is not occluded in microaggregates or micropores, nor is it associated with minerals, all of which are mechanisms that protect MAOC from climate change²⁶. Due to the typically lower carbon quality of POC²⁷, the “carbon-quality temperature” hypothesis suggests that the decomposition of low-quality substrates requires higher activation energy, making it more sensitive to temperature changes^{28,29}. In contrast, the decomposition of MAOC is less sensitive to temperature because mineral protection limits microbial decomposers and their enzymes’ access to MAOC, resulting in a slower decomposition rate compared to that of POC³⁰. Consequently, studies have found that the Q_{10} of POC is higher than that of MAOC^{25,27,31}. However, the impact of warming on the Q_{10} of POC and MAOC remains unclear. Since warming can enhance microbial activity and increase the utilization of labile carbon, leading to a decline in substrate quality of POC³², we hypothesize that warming will increase the Q_{10} of POC while having a minimal effect on the Q_{10} of MAOC.

To test this hypothesis, we conducted a 3-year *in situ* warming experiment at 12 abandoned cropland sites located in different climatic zones of China, with latitudes ranging from 22.33 to 46.58°N, mean annual temperatures ranging from -0.9 to 22.3 °C, and mean annual precipitation ranging from 330 to 2272 mm (Fig. 1, Supplementary Table 1). Physical fractionation of SOC and incubation experiment under varying temperatures were employed to explore the effects of warming on POC and MAOC content as well as their Q_{10} , and the surrounding biotic and abiotic influencing factors were analyzed to uncover the underlying mechanisms.

Results and Discussion

The changes in POC and MAOC in surface soils under warming

On average, surface (0–15 cm) soil temperature significantly increased by 1.6 °C whereas soil moisture significantly decreased by 4.7% across 12 sites after 3-year simulated warming (all $P < 0.01$, Supplementary Fig. 1). In the control treatment, SOC content ranged from 4.9 to 32.5 g kg⁻¹ at the 12 sites (Fig. 1); POC and MAOC content ranged from

1.3 to 13.4 g kg⁻¹, and 2.3 to 17.3 g kg⁻¹, respectively, with average POC and MAOC content of 6.1 g kg⁻¹ and 6.6 g kg⁻¹, respectively (Fig. 1). Warming had no significant effect on SOC content ($P > 0.05$, Fig. 1), with the POC content not significantly altered ($P > 0.05$, Fig. 1) while the MAOC content significantly increased under warming ($P < 0.01$, Fig. 1). Therefore, the average ratio of MAOC to SOC increased under warming (from 0.45 to 0.48, Fig. 1). Moreover, the aromaticity (ratio of peak value at 1620 cm⁻¹ to the sum of peak values at 2850 cm⁻¹ and 2920 cm⁻¹ from FTIR spectrum, $r_{1620}/(2850 + 2920)$) of POC significantly increased under warming ($P < 0.01$, Supplementary Fig. 2), indicating a significant decline in the carbon quality of POC under warming.

Key factors regulating the changes in POC and MAOC content under warming

We investigated the impact of changes in biotic and abiotic influencing factors on the changes in POC and MAOC content under warming. Firstly, Pearson correlation analysis indicated that the change in POC content was significantly positively correlated with the changes in soil temperature, root biomass (RB), and POC fungal α -diversity (reflected by Shannon index) under warming, respectively (all $P < 0.05$, Supplementary Fig. 3). The change in MAOC content was significantly positively related with the changes in pedogenic iron oxides (Fe_d) and MNC under warming, respectively (all $P < 0.05$, Supplementary Fig. 3). Then, the results of Random Forest analysis revealed that changes in RB and MNC were the main factors influencing the changes in POC and MAOC content, respectively (Fig. 2), which suggested that the changes in POC and MAOC content were primarily influenced by changes in their respective inputs under warming¹⁷.

Warming promoted plant growth in abandoned croplands, as evidenced by the increase in RB under warming ($P < 0.01$, Supplementary Fig. 4). The carbon input from grass-dominated abandoned croplands (Supplementary Table 1) is readily transformed by microorganisms¹⁶, leading to a significant increase in MNC content ($P < 0.05$, Supplementary Fig. 4). Moreover, fungi typically exhibit higher carbon utilization efficiency, allocating more organic matter towards their own growth³³. The significant increase in fungal biomass under warming ($P < 0.05$, Supplementary Fig. 5) might be one of the reasons for the increase in MNC content (Supplementary Fig. 4). The increase in microbially-derived carbon input can enhance MAOC content under warming (Fig. 1). In addition to increased input, the increase in Fe_d under warming ($P < 0.01$, Supplementary Fig. 4) might also contribute to the increase in MAOC content. The accumulation of decomposition products from litter and root exudates could lead to an increase in acidic substances in the soil under warming³⁴, resulting in a decrease in soil pH ($P < 0.01$, Supplementary Fig. 4). The significant increase in soil oxalic acid content under warming ($P < 0.05$, Supplementary Fig. 6), and the significant negative correlation between the changes in oxalic acid content and pH under warming ($P < 0.01$, Supplementary Fig. 6), provided evidence for this phenomenon. The decline in pH was beneficial for the increased solubility of hydrolyzed cations such as Fe^{3+} ³⁵. Meanwhile, warming could reduce soil moisture (Supplementary Fig. 1) and then increase soil oxygen levels, which was conducive to the conversion of Fe^{2+} into Fe^{3+} in the soil³⁶. These processes could significantly increase Fe_d content (Supplementary Fig. 4), enhancing the sorption capacity of minerals for SOC³⁷. For POC, despite the increased RB under warming (Supplementary Fig. 4), the enhanced microbial decomposition and transformation of OC may lead to a balance between the input and output of the POC pool under warming, resulting in maintained POC content (Fig. 1).

Changes in Q_{10} of POC and MAOC under warming, along with the driving factors

The Q_{10} of POC was significantly higher than that of MAOC in the control treatment ($P < 0.01$, Fig. 3). Some previous carbon-climate

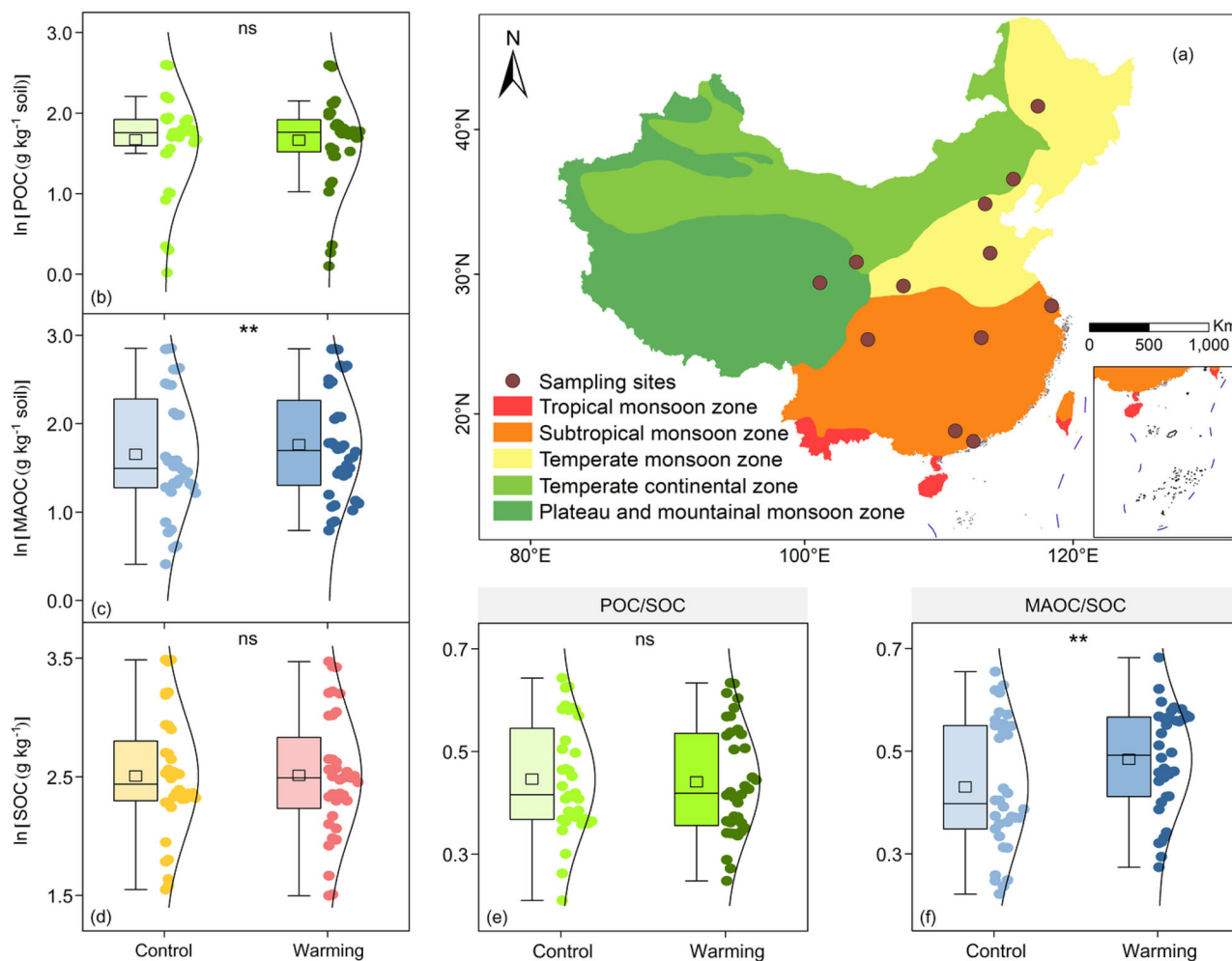


Fig. 1 | Locations of the field warming experiment at 12 sites in abandoned croplands in China (a), along with changes in particulate, mineral-associated, and soil organic carbon (POC, MAOC, and SOC) content (b, c, and d), and the ratios of POC or MAOC to SOC (POC/SOC and MAOC/SOC, e and f) under warming. POC and MAOC content is \log_e (ln) transformed. The ends of boxplots

represent the 25th and 75th percentiles. Within each boxplot, the horizontal line and box symbolize the median and mean, respectively, and error bars represent the standard deviation. n = 36 per treatment (i.e., 12 × 3; 3 is the replication from the sampling sites). **, $P < 0.01$; ns, $P > 0.05$.

feedback models assumed a constant value for Q_{10} ^{38,39}, however, in recent years, more and more studies have questioned this assumption^{22,28,40}. Therefore, we further investigated the effects of warming on the Q_{10} of POC and MAOC. The results indicated a tendency for an increase (although not significant) in the Q_{10} of POC, while the Q_{10} of MAOC remained unchanged under warming (Fig. 3).

Subsequently, we explored the key influencing factors affecting the changes in POC and MAOC Q_{10} under warming. The results of Pearson correlation analysis showed that the change in POC Q_{10} was significantly negatively correlated with the changes in pH, lignin content, and POC r1620/(2850 + 2920), while the change in MAOC Q_{10} to warming was significantly negatively related with the change in organic-complexed iron (Fe_p) under warming (all $P < 0.05$, Supplementary Fig. 7). The Random Forest analysis revealed that the changes in POC r1620/(2850 + 2920) and Fe_p were the predominant factors affecting the changes in POC and MAOC Q_{10} , respectively (Fig. 4), which indicated that warming affected the Q_{10} of POC and MAOC through changes in carbon quality and mineral protection, respectively.

Warming increased microbial biomass (Supplementary Fig. 5), enhancing the utilization of labile carbon³², leading to a decline in the carbon quality of POC (Supplementary Fig. 2). SOC with lower quality require higher activation energy to break chemical bonds during

decomposition, and warming can provide additional energy to promote the decomposition process, making it more sensitive to temperature^{28,29}. Where warming decreased the carbon quality of POC, it increased its Q_{10} under warming.

The negative correlation between the change in Fe_p and the change in MAOC Q_{10} under warming implied that stronger mineral protection mainly led to lower Q_{10} of MAOC (Supplementary Fig. 7), consistent with the “mineral protection” hypothesis^{41,42}. Metal oxides can provide protection to MAOC through the following mechanisms: firstly, metal oxides can act as connective cements to promote the formation of soil aggregates. This process can limit the access of microorganisms and their enzymes into the soil aggregates⁴³, while also altering soil porosity and restricting oxygen diffusion⁴⁴, consequently leading to the physical protection of MAOC; secondly, metal oxides can form complexes with organic compounds through covalent or electrostatic bonds, creating stable complexes that are less susceptible to microbial decomposition, which is because microorganisms require additional energy to break the complexes to utilize such carbon⁴⁵; thirdly, metal oxides have a strong sorption capacity for extracellular enzymes involved in SOC decomposition, leading to enzyme inactivation and inhibiting microbial decomposition of organic compounds⁴¹. In conclusion, mineral protection can affect the Q_{10} of MAOC through microbial inhibition and spatial constraints^{46,47}.

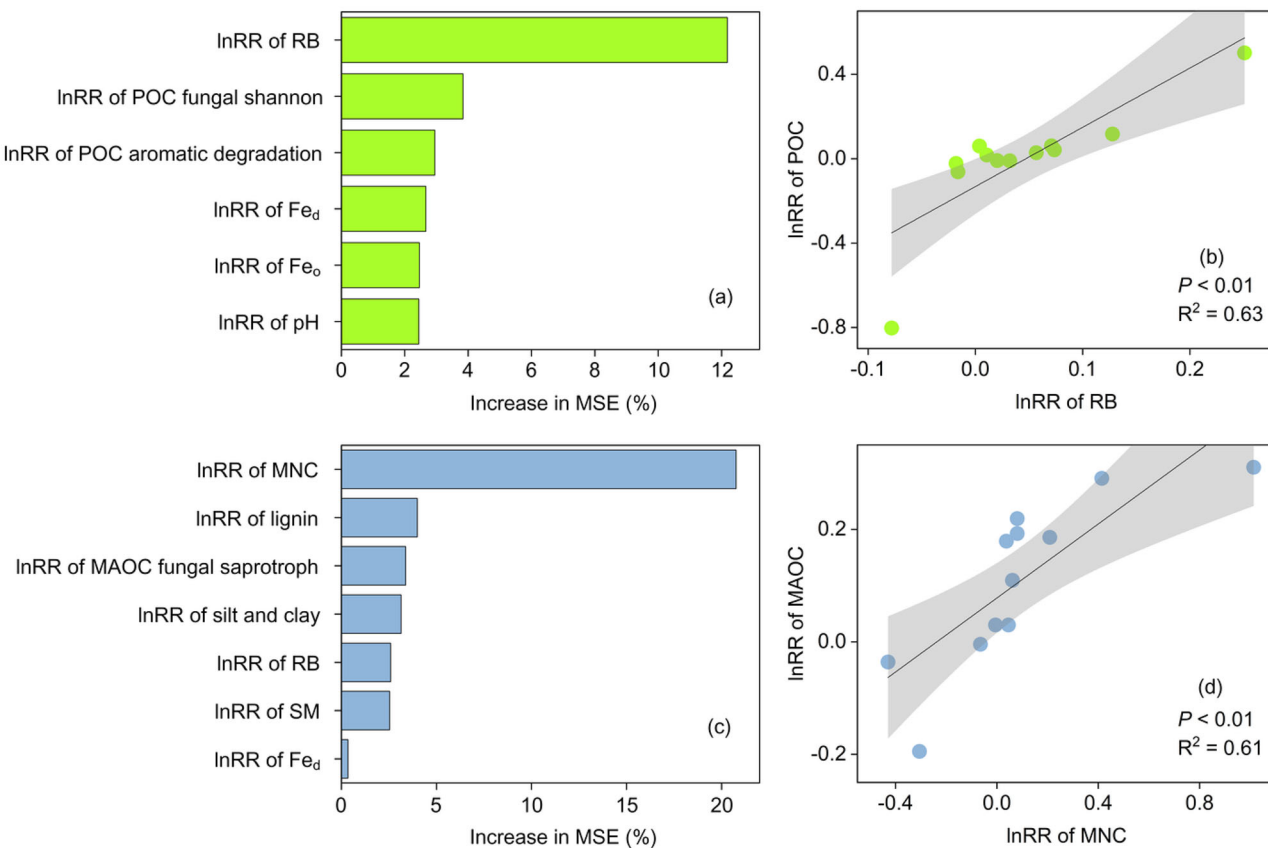


Fig. 2 | The relationship between the response ratio (InRR) of particulate and mineral-associated organic carbon (POC and MAOC) content with the InRR of potential driving factors under warming. **a, c** The relative importance of the InRR of influencing factors in affecting the InRR of POC and MAOC content derived by Random Forest model. **b** Relationship between the InRR of POC content and the InRR of root biomass (RB). **d** Relationship between the InRR of MAOC content and

the InRR of microbial necromass carbon (MNC). POC aromatic degradation: bacteria involved in aromatic compound degradation of POC; Fe_d and Fe_o : pedogenic iron oxides and poorly crystalline iron oxides; SM: soil moisture. $n = 12$, where the POC aromatic degradation, POC fungal Shannon, and MAOC fungal saprotroph parameters represent composite samples of the sampling sites, and the other parameters represent the mean values of replicate samples from the sampling sites.

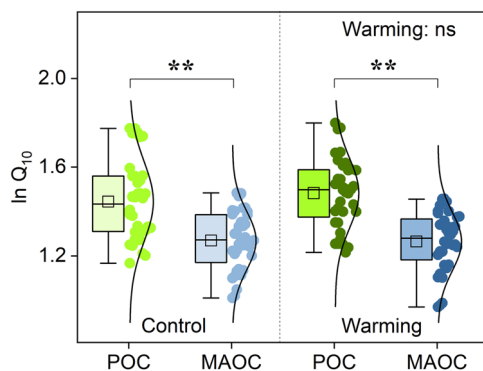


Fig. 3 | Difference in temperature sensitivity (Q_{10}) between particulate and mineral-associated organic carbon (POC and MAOC) in warming and control treatments. All variables are log_e (ln) transformed. The ends of boxplots represent the 25th and 75th percentiles. Within each boxplot, the horizontal line and box symbolize the median and mean, respectively, and error bars represent the standard deviation. $n = 36$ per treatment (i.e., 12×3 ; 3 is the replication from the sampling sites). **, $P < 0.01$; ns, $P > 0.05$.

Warming significantly increased Fe_p ($P < 0.01$, Supplementary Fig. 4), enhancing mineral protection and resulting in MAOC decomposition insensitive to warming (Fig. 3). However, the Q_{10} value of MAOC remained unchanged (but was greater than 1) under warming, indicating that warming could still enhance the decomposition of MAOC

(Fig. 3). The increase in inputs might be disproportionately larger than increase in decomposition, resulting in an overall increase in MAOC content (Fig. 1).

Implications for soil carbon management in croplands under climate warming

Our findings hold significant practical implications for cropland management under climate warming. Previous studies have consistently indicated that the natural recovery process by secondary succession could increase the SOC content in abandoned croplands^{3,19}; yet, the specific SOC fraction primarily influenced by this conversion, especially under conditions of climate warming, remains uncertain. Our results indicated that POC content remained unchanged while MAOC content significantly increased in abandoned croplands under warming and increased input of labile plant-derived carbon (Figs. 1 and 5). The Q_{10} of MAOC was significantly lower than that of POC regardless of the warming or control treatment (Fig. 3), which suggested that MAOC represented the most persistent and least vulnerable carbon fraction within SOC. Based on this observations and previous estimates of the area of abandoned croplands in China (approximately 392,156.2 km²)⁷, we speculated on the potential impact of short-term warming on POC and MAOC stocks in the surface soils (0–15 cm) of these croplands (considering that soil bulk density was not significantly changed under warming ($P > 0.05$, Supplementary Fig. 8)). The estimates suggested that short-term warming led to an increase of 0.04 Pg C in MAOC stock, which is double the increase observed in POC stock (0.02 Pg C, due to changes in soil particle size under warming, the POC stock

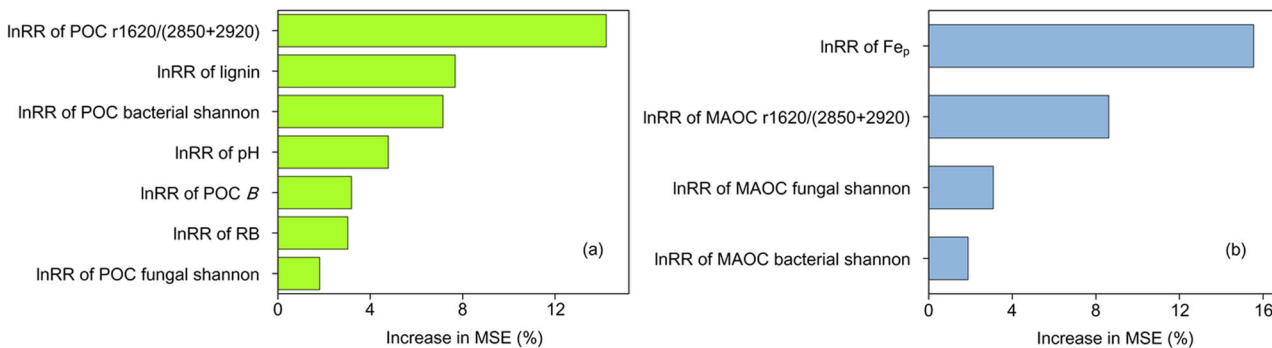


Fig. 4 | The relative importance of the response ratio (InRR) of influencing factors in affecting the InRR of particulate and mineral-associated organic carbon (POC and MAOC, a and b) temperature sensitivity (Q_{10}) derived by Random Forest model. POC or MAOC r1620/(2850 + 2920): ratio of peak value at 1620 cm^{-1} to the sum of peak values at 2850 cm^{-1} and 2920 cm^{-1} from FTIR

spectrum of POC or MAOC; POC B: the fundamental microbial respiration rate of unit OC at 0 $^{\circ}\text{C}$ of POC; RB: root biomass. $n=12$, where the POC or MAOC r1620/(2850 + 2920), POC or MAOC bacterial and fungal Shannon parameters represent composite samples of the sampling sites, and the other parameters represent the mean values of replicate samples from the sampling sites.

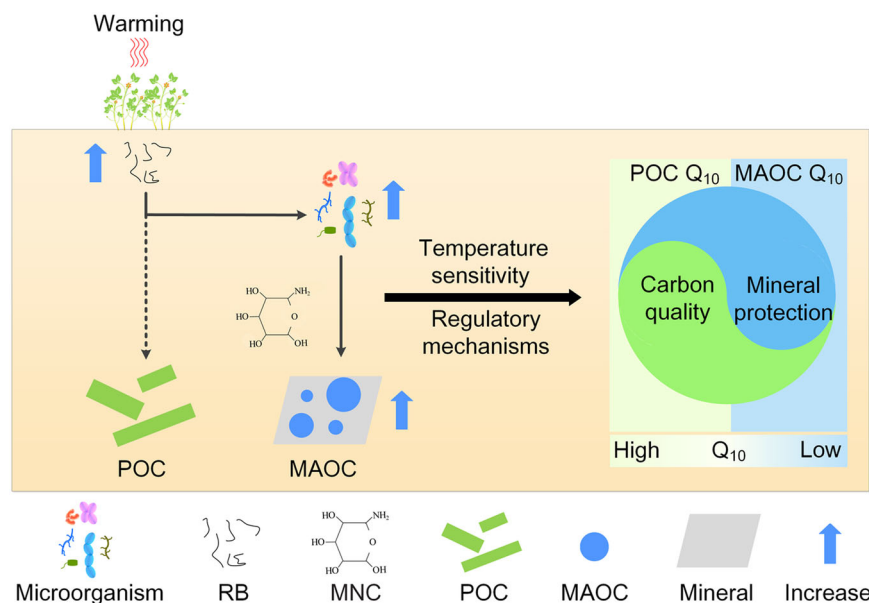


Fig. 5 | Conceptual diagram illustrating the response of particulate and mineral-associated organic carbon (POC and MAOC) to warming and the regulatory mechanisms of temperature sensitive (Q_{10}) of POC and MAOC. RB: root biomass; MNC: microbial necromass carbon.

increased despite no significant changes in POC content or bulk density). This suggested that short-term warming was more conducive to the accumulation of stable carbon in abandoned croplands. However, based on the “soil carbon saturation” hypothesis, minerals exhibit a saturation threshold for binding SOC¹⁰. When the MAOC content reaches saturation, continuously inputting plant-derived carbon may increase the content of POC²¹. Therefore, it is imperative to assess whether the MAOC content has reached saturation in the warming treatment.

The carbon saturation capacity of the 12 sites was estimated using the regression equations reported by Hassink⁴⁸ and Six⁴⁹, respectively, and compared them with the MAOC content in the warming treatment. The results indicated that, except for the Maqin site (located on the Qinghai-Tibet Plateau, abandoned for over 10 years, reaching approximately 60–80% of estimated carbon saturation capacity), the MAOC content in other sites was <50% of the estimated carbon saturation capacity (Supplementary Fig. 9). This suggested that the MAOC content in the warming treatment had not yet reached saturation in this study. Moreover, a 10-year in situ warming experiment (+2 $^{\circ}\text{C}$) reported that warming significantly increased SOC content in croplands, which was attributed to a significant increase in MNC³;

consistent with numerous previous studies, including our study, which showed a significant positive correlation between MNC and MAOC content^{13,50}, the result might imply that a decade of warming could potentially lead to an increase in MAOC content in abandoned croplands. Furthermore, we found that Fe_d, Fe_p, and silt and clay content increased under warming (Supplementary Fig. 4), suggesting that warming may have created more potential sites for mineral sorption of MAOC³⁷.

However, whether long-term warming necessarily leads to an increase in MAOC content remains a subject of debate. Several studies have shown a significant negative correlation between MAOC content and mean annual temperature^{26,51}, indicating that warming could reduce MAOC content. This phenomenon is partly due to the enhanced microbial decomposition of MAOC under warming^{27,51}. Meanwhile, since the desorption of SOC from minerals is generally an endothermic reaction, warming can promote this process, further decreasing MAOC content⁵². This suggests that the apparent MAOC capacity is constrained by environmental covariates, such as management practices and climate, because it results from a balance between inputs and outputs. Therefore, in theory, even if warming would increase the sorption sites for MAOC, the apparent MAOC

capacity might still decrease. Although warming can accelerate MAOC accumulation in the short term, long-term warming may reduce soil MAOC stock, ultimately limiting overall carbon sequestration and increasing positive carbon feedback to climate change. More research is needed to understand the changes in different SOC fractions in abandoned croplands over longer time scales under warming, to optimize management practices and promote soil carbon sequestration.

Methods

Study sites and field warming experiment

Croplands that have remained uncultivated for five consecutive years is typically defined as abandoned croplands⁷. Based on previous investigations, we conducted a field warming experiment across 12 abandoned croplands in China investigate the impact of warming on different fractions of soil organic carbon (SOC). The sampling sites were distributed within latitude ranging from 22.33°N to 46.58°N, mean annual temperatures (MAT) spanning from -0.9 °C to 22.3 °C, and mean annual precipitation (MAP) ranging from 330 mm to 2272 mm (Fig. 1, Supplementary Table 1). The primary reason for the abandonment of these croplands is the decline in soil fertility, as indicated by SOC content (Supplementary Table 1). Currently, these croplands are undergoing natural recovery by secondary succession.

Since July 2018, simulated warming experiments have been conducted at each sampling site using open-top chambers (OTCs). See Supplementary Method 1 for details of the OTCs. The experiment consisted of six plots, including three warming and three control treatments (labeled as “warming” and “control” respectively). Each plot had an area of 2 m × 2 m, with buffer distances of 2–3 m between adjacent plots. The topography and plant composition were similar between warming and control treatments at each site. From July 2018 to July 2021, soil temperature and moisture were measured three times a year in the surface soil (0–15 cm) in April, July, and November. The simulated warming experiments led to an average temperature increase of 1.6 °C in the surface soil at the 12 sites (Supplementary Fig. 1). The soil type classification is based on the international standard for soil classification system, the World Reference Base (WRB).

Soil sampling and analyses

In July 2021, surface soil samples were collected from each warming and control plot at the 12 sites. Three soil cores were randomly taken from each plot using a 5 cm diameter soil auger and thoroughly mixed to form composite samples, resulting in a total of 72 soil samples collected (12 sites × 2 treatments × 3 plots). The collected soil samples were transported to the laboratory using ice packs and subsequently divided into two parts: one portion of soil samples was air-dried, sieved through a 2 mm mesh for measuring soil physicochemical properties and for separating POC and MAOC; the other portion was stored at -80 °C for further microbial analysis. Furthermore, a 15 cm deep soil core was randomly collected from each plot for measuring root biomass (RB). In each plot, soil samples were randomly collected using a 100 cm³ ring cutter to determine soil bulk density⁵³, and therefore, three samples were collected from warming and control treatments in each site, respectively.

SOC content was measured using the potassium dichromate oxidation method⁵⁴. Soil pH was determined under the condition of a 1:2.5 ratio of water to soil (SL1000, HACH, USA)⁵⁴. Soil texture analysis was carried out using the hydrometer method (sand 2–0.02 mm, silt 0.02–0.002 mm, and clay <0.002 mm)⁵⁴. For the analysis of iron oxides, including crystalline iron (Fe_d), poorly crystalline iron (Fe_o), and organic-complexed iron (Fe_p), extractions were performed using solutions of citrate-carbonate-dithionite, ammonium oxalate, and sodium pyrophosphate solutions, respectively³⁷. Subsequently, the concentrations of iron elements in the solutions were determined using an inductively coupled plasma optical emission spectrometer

(ICP-OES, Optima 8300, USA). Oxalic acid in soil was extracted using a phosphate buffer, and then quantified using high-performance liquid chromatography (HPLC, 1260 Infinity LC; Agilent Technologies, Santa Clara, CA, USA)⁵⁵. Two groups of biomarkers, amino sugars (summarized as glucosamine, galactosamine, and muramic acid) and lignin (summarized as vanillin, acetovanillone, vanillic acid, syringaldehyde, acetosyringone, syringic acid, *p*-coumaric acid, and ferulic acid), were employed to trace microbial necromass carbon (MNC) and plant-derived carbon, respectively^{56,57}. See Supplementary Methods 2 and 3 for detailed measurements of amino sugars and lignin, respectively.

SOC fractionation

We fractionated SOC based on particle size^{10,11}. Briefly, 100 g of air-dried and sieved soil from each plot were thoroughly dispersed in a 0.5% solution of sodium hexametaphosphate (500 ml) with microbeads, by shaking for 18 h. The dispersed soil was subsequently rinsed over a 53 µm sieve, and the portion passing through (<53 µm) was collected as mineral-associated organic matter (MAOM), while the remaining portion on the sieve was collected as particulate organic matter (POM). POM and MAOM were soaked in ultrapure water and centrifuged three times, respectively, to remove sodium hexametaphosphate. After being dried to a consistent weight in an oven at 40 °C, the OC content in both POM and MAOM (i.e., POC and MAOC) was determined using the potassium dichromate method.

Laboratory incubation for temperature sensitivity (Q₁₀)

Since constant incubation temperature may cause microorganisms to adapt to the corresponding temperature by producing new enzymes or altering membrane fatty acids, potentially influencing the Q₁₀ of SOC^{40,58}, we conducted an incubation experiment under varying temperatures to explore the CO₂ release rate of POC and MAOC. Specifically, 20 g POC or MAOC from each plot were weighed into 250 ml glass bottles. Considering the potential influence of the introduced sodium hexametaphosphate during the fractionation process on the microbial community, an inoculum of the original soil was prepared (add 1 g of dry weight fresh soil to 100 ml of sterilized ultrapure water and fully shaken, filtered through a Whatman GF/C filter²²) before the cultivation experiment. Then, the inoculum was added to the glass bottles containing the weighed POC or MAOC samples (0.4 ml per gram samples²²), and further adjusted with ultrapure water to achieve 60% of water-holding capacity. Subsequently, the samples were pre-incubated at 20 °C for 10 days. Moreover, three empty bottles were incubated as blanks.

After the pre-incubation, the incubation temperature first started from 5 °C, gradually increased to 25 °C with 5 °C as a step, and then gradually decreased from 25 °C to 5 °C with the same step⁵⁹. After each temperature adjustment, a 3 h equilibration period was implemented to allow POC or MAOC samples to adapt to the changing temperature conditions. To maintain a consistent soil moisture content, deionized water was added when water loss reached 0.1 g. After the equilibration period, the cultivation bottles were purged with CO₂-free air for 5 min and then sealed for incubation. Based on preliminary experiments, the incubation time was determined: 35, 20, 10, 6, and 4 h for temperatures of 5, 10, 15, 20, and 25 °C, respectively. After the incubation period, 10 mL of gas was collected from the headspace of each bottle using a syringe. The concentration of CO₂ in the collected gas was measured using a gas chromatograph (Agilent 7890B, California, USA). By subtracting the blank values, the CO₂ release of POC and MAOC were obtained.

Carbon quality characterization of POC and MAOC

Due to the similar soil physicochemical properties among the three plots within each treatment group (Supplementary Table 2), the samples from the three plots were uniformly combined into a single sample before measuring the carbon quality of POC and MAOC, resulting in 24 samples (12 for warming treatment and 12 for control

treatment) for both POC and MAOC, respectively. The carbon functional groups in POC and MAOC were analyzed using a Fourier-transform infrared spectrometer (FTIR, NEXUS 670, OSIC, USA). Briefly, 2 mg of POC or MAOC samples were homogeneously mixed with 180 mg of potassium bromide to form pellets. Scans were conducted in the range of 4000 to 400 cm^{-1} at a resolution of 4 cm^{-1} , with a scan frequency of 50 times. The spectra were baseline-corrected, and then the ratio of peak value at 1620 cm^{-1} to the sum of peak values at 2850 cm^{-1} and 2920 cm^{-1} was calculated ($r_{1620}/(2850 + 2920)$) to determine the carbon quality of POC and MAOC⁴¹. A higher $r_{1620}/(2850 + 2920)$ indicates higher aromaticity and lower carbon quality⁴¹.

Microbial property analysis

Similar to the carbon quality analysis of POC and MAOC, microbial biomass and α -diversity were analyzed for 24 bulk soil samples, with corresponding analyses of microbial α -diversity for POC and MAOC fractions. We employed the phospholipid fatty acid (PLFA) extraction method recommended by Bossio and Scow⁶⁰ to measure soil microbial biomass. See Supplementary Method 4 for details of the PLFA extraction and analysis. We calculated the bacterial (i14:0, a15:0, i15:0, i16:0, 16:1 ω 7c, a17:0, cy17:0, i17:0, 18:1 ω 7, cy19:0) and fungal (18:2 ω 6, 9c) PLFAs, respectively^{22,61}.

Bacterial and fungal community structure and α -diversity of bulk soil, as well as POC and MAOC, were determined through sequencing of the 16S and ITS rRNA genes^{41,62}. It is noteworthy that, to avoid the effects of sodium hexametaphosphate on microorganisms, gene sequencing of POC and MAOC was conducted on samples that were inoculated and incubated at 20 °C for 10 days (mentioned in laboratory incubation).

Based on the manufacturer's guidelines, DNA was extracted from bulk soil, POC, and MAOC using the PowerSoil DNA Isolation Kit (MoBio Laboratories Inc., Carlsbad, CA, USA), with a sample weight of 0.5 g. The initial evaluation of DNA quality was performed with the NanoDrop 8000 UV-Vis spectrophotometer (Thermo Fisher Scientific, Madison, USA). Subsequently, DNA concentration was determined using the QubitTM 3.0 Fluorometer (Life Technologies, Grand Island, NY, USA). High-throughput sequencing analysis was executed utilizing the 515 F (5'-GTGCCAGCMGCCGCGTAA-3') and 806 R (5'-GGAC-TACHVGGGTWTCTAAT-3') primers for bacterial community assessment and the ITS3F (5'-GCATCGATGAAGAACCGCAGC-3') and ITS4R (5'-TCCTCCGCTTATTGATATGC-3') primers for fungal community evaluation⁶². The sequencing procedure was managed by Majorbio BioPharm Technology Co., Ltd., employing the Illumina Nova 6000 platform in accordance with standard protocols⁶³. Briefly, polymerase chain reaction (PCR) was employed for amplification, followed by assessment of PCR product concentration and length via 1% agarose gel electrophoresis. Subsequent to mixing and purification of PCR products using the ENZA Gel Extraction Kit (Omega Bio-Tek Corporation, Norcross, Georgia, USA), DNA library preparation utilized the NEBNext® Ultra DNA Library Prep Kit for Illumina (New England Biolabs, Ipswich, Massachusetts, USA). Evaluation of library quality was conducted through the Qubit 3.0 Fluorometer and the Agilent 4200 TapeStation system (Agilent, Santa Clara, CA). Sequencing was carried out using the Illumina Nova 6000 platform, producing paired-end reads with a length of 2 × 250 base pairs.

Magigene Cloud Platform (<http://cloud.magigene.com>) was employed to analyze the sequencing data. Initial assessment of raw data quality was conducted using the fastp software, with primer sequences being eliminated utilizing the cutadapt software. The quality-filtered sequences derived from the 16S and ITS rRNA gene were grouped into Operational Taxonomic Units (OTUs) at a 97% similarity cutoff. The most frequently occurring sequence within each OTU was designated as the representative sequence, achieved by utilizing the ribosomal database project classifier. Taxonomic annotation of sequences was performed using the basic local alignment search

tool. All samples were normalized to the smallest sequence number through rarefaction. The Shannon index was used to evaluate the α -diversity of the bacterial and fungal community⁶⁴. Moreover, the FAPROTAX and FUNGuild tools were employed to predict bacterial and fungal functions according to the taxonomic information of OTUs, respectively⁶². Based on functional predictions, the relative abundance of fungal saprotroph was found to be the highest in both POC and MAOC (Supplementary Fig. 10), and therefore was selected for subsequent analysis.

Data analysis

The decomposition rate of organic carbon is calculated using the following formula⁵⁹:

$$R = V \times (C_s - C_b) \times 273 / ((273 + T) \times 22.4) \times M / (W \times t) \quad (1)$$

where R is the CO_2 release rates ($\mu\text{g C-CO}_2 \text{ g}^{-1} \text{ h}^{-1}$) at a given temperature ($T, ^\circ\text{C}$), V is the headspace volume in the incubation bottle (L), C_s and C_b represent the CO_2 gas concentrations in soil samples and blank incubation bottles (ppm), respectively, M represents the molecular weight of CO_2 , W is the mass of soil used for incubation (dry weight, g), and t represents the sealing time of the incubation bottles (h).

A commonly used exponential function (Eq. 2) was employed to analyze the relationship between CO_2 release rates of both POC and MAOC and temperature^{59,65,66}:

$$R = Be^{kT} \quad (2)$$

where B and k are the fit parameters. The parameter "B" represents the fundamental microbial respiration rate of unit OC at 0 °C.

Q_{10} value was employed to describe the temperature sensitivity of POC and MAOC calculated as follows:

$$Q_{10} = e^{10k} \quad (3)$$

The fitted parameters of POC and MAOC were listed in Supplementary Tables 3 and 4.

We calculated the density of POC (POCD) or MAOC (MAOCD) in the surface soil of abandoned croplands according to Eq. (4) (kg C m^{-2})^{54,67}:

$$\text{POCD or MAOCD} = A \times BD \times OC \times (1 - C/100)/100 \quad (4)$$

where A represents soil thickness (cm), BD is bulk density (g cm^{-3}), OC represents organic carbon of POC or MAOC (g kg^{-1}), and C is percentage of the fraction $> 2 \text{ mm}$, respectively.

The POC or MAOC stock (POC_{stock} or MAOC_{stock}, Tg C) in surface soil was subsequently calculated using the following equation^{54,67}:

$$\text{POC}_{\text{stock}} \text{ or } \text{MAOC}_{\text{stock}} = \text{POCD or MAOCD} \times S/1000 \quad (5)$$

where S represents the soil area of abandoned croplands in China, which is 392,156.2 km^2 , as determined by a recent study⁷.

The carbon saturation capacity (CSC, g kg^{-1}) at the 12 sites was estimated based on the regression equation reported by Hassink (CSC_{Hassink})⁴⁸ and Six (CSC_{Six})⁴⁹:

$$\text{CSC}_{\text{Hassink}} = 4.09 + 0.37 \times \text{the percentage of silt and clay} (R = 0.89) \quad (6)$$

$$\text{CSC}_{\text{Six}} = 4.38 + 0.26 \times \text{the percentage of silt and clay} (R = 0.41) \quad (7)$$

where the percentage of silt and clay (%) used in the regression equations represents the average value in the warming treatment.

Statistical analyses

Before analysis, natural logarithm (ln) transformation of the data was carried out when required to fulfill the assumption of normality. Linear mixed effects models (LMMs, “nlme” package) were employed to investigate differences in POC, MAOC content and Q_{10} , as well as biotic and abiotic influencing factors with three replicates (including soil temperature, soil moisture, RB, SOC, Fe_{d} , Fe_{o} , Fe_{p} , pH, silt and clay, lignin, MNC, and bulk density) among different treatments (i.e., warming and control treatments). These variables were fitted as fixed factors, and plots nested within the site were fitted as random factors. Tukey's test (“multcomp” package) was conducted for further analysis of significant differences among variables between different treatments. Moreover, paired t test was employed to assess the differences in other influencing factors, including bulk soil bacterial and fungal PLFAs, bacterial and fungal α -diversity, as well as POC and MAOC bacterial and fungal α -diversity and the POC and MAOC r1620/(2850 + 2920) ratio, among different treatments.

We evaluated the response of variables to warming using the natural logarithm of the response ratio (lnRR)⁶⁸:

$$\lnRR = \ln(X_w/X_c) = \ln(X_w) - \ln(X_c) \quad (8)$$

where X_w and X_c are the arithmetic mean values of the variables in warming and control treatments, respectively.

Pearson correlation analysis and ordinary least squares linear regression analysis were employed to assess the relationship between the lnRR of potential biotic and abiotic factors with the lnRR of the content and Q_{10} of POC and MAOC. Then, by employing a Random Forest model (“randomForest” package), we investigated the relative importance of the lnRR of influencing factors on the lnRR of content and Q_{10} of POC and MAOC. The statistical analysis was carried out using Statistical Product and Service Solutions 20 (SPSS 20.0) and R 4.3.2.

Reporting summary

Further information on research design is available in the Nature Portfolio Reporting Summary linked to this article.

Data availability

All data used in this study could be downloaded from the Figshare database (<https://doi.org/10.6084/m9.figshare.25816564>). The sequencing data obtained in this study have been submitted to the NCBI Sequence Read Archive (SRA) and are available under the accession number PRJNA1194767 and PRJNA1194782. Source data are provided with this paper.

References

1. Sanderman, J., Hengl, T. & Fiske, G. J. Soil carbon debt of 12,000 years of human land use. *Proc. Natl. Acad. Sci. USA* **114**, 9575–9580 (2017).
2. Schuur, E. A. G. et al. Climate change and the permafrost carbon feedback. *Nature* **520**, 171–179 (2015).
3. Tian, J. et al. Microbially mediated mechanisms underlie soil carbon accrual by conservation agriculture under decade-long warming. *Nat. Commun.* **15**, 377 (2024).
4. Prairie, A. M., King, A. E. & Cotrufo, M. F. Restoring particulate and mineral-associated organic carbon through regenerative agriculture. *Proc. Natl. Acad. Sci. USA* **120**, e2217481120 (2023).
5. Roccia, K. S., Lavallee, J. M., Stewart, C. E. & Cotrufo, M. F. Soil organic carbon response to global environmental change depends on its distribution between mineral-associated and particulate organic matter: a meta-analysis. *Sci. Total. Environ.* **793**, 148569 (2021).
6. Zheng, Q. et al. The neglected role of abandoned cropland in supporting both food security and climate change mitigation. *Nat. Commun.* **14**, 6083 (2023).
7. Zhang, M. et al. Reveal the severe spatial and temporal patterns of abandoned cropland in China over the past 30 years. *Sci. Total. Environ.* **857**, 159591 (2023).
8. Gao, H., Xia, X., Zhang, Z., Chen, J. & Liu, S. Temperature response of soil respiration decreases with latitude and elevation in abandoned croplands. *Agr. Ecosyst. Environ.* **363**, 108862 (2024).
9. Sokol, N. W. et al. Global distribution, formation and fate of mineral-associated soil organic matter under a changing climate: A trait-based perspective. *Funct. Ecol.* **36**, 1411–1429 (2022).
10. Cotrufo, M. F., Ranalli, M. G., Haddix, M. L., Six, J. & Lugato, E. Soil carbon storage informed by particulate and mineral-associated organic matter. *Nat. Geosci.* **12**, 989–994 (2019).
11. Lugato, E., Lavallee, J. M., Haddix, M. L., Panagos, P. & Cotrufo, M. F. Different climate sensitivity of particulate and mineral-associated soil organic matter. *Nat. Geosci.* **14**, 295–300 (2021).
12. Hall, S. J., Ye, C., Weintraub, S. R. & Hockaday, W. C. Molecular trade-offs in soil organic carbon composition at continental scale. *Nat. Geosci.* **13**, 687–692 (2020).
13. Zhang, Z., Kaye, J. P., Bradley, B. A., Amsili, J. P. & Suseela, V. Cover crop functional types differentially alter the content and composition of soil organic carbon in particulate and mineral-associated fractions. *Glob. Chang. Biol.* **28**, 5831–5848 (2022).
14. Chen, S. et al. Plant diversity enhances productivity and soil carbon storage. *Proc. Natl. Acad. Sci. USA* **115**, 4027–4032 (2018).
15. Cotrufo, M. F., Wallenstein, M. D., Boot, C. M., Denef, K. & Paul, E. The Microbial Efficiency-Matrix Stabilization (MEMS) framework integrates plant litter decomposition with soil organic matter stabilization: do labile plant inputs form stable soil organic matter? *Glob. Change Biol.* **19**, 988–995 (2013).
16. Camenzind, T., Mason-Jones, K., Mansour, I., Rillig, M. C. & Lehmann, J. Formation of necromass-derived soil organic carbon determined by microbial death pathways. *Nat. Geosci.* **16**, 115–122 (2023).
17. Lavallee, J. M., Soong, J. L. & Cotrufo, M. F. Conceptualizing soil organic matter into particulate and mineral-associated forms to address global change in the 21st century. *Glob. Change Biol.* **26**, 261–273 (2020).
18. Cotrufo, M. F. et al. Formation of soil organic matter via biochemical and physical pathways of litter mass loss. *Nat. Geosci.* **8**, 776–779 (2015).
19. Seabloom, E. W., Borer, E. T., Hobbie, S. E. & MacDougall, A. S. Soil nutrients increase long-term soil carbon gains threefold on retired farmland. *Glob. Chang. Biol.* **27**, 4909–4920 (2021).
20. Rui, Y. et al. Persistent soil carbon enhanced in Mollisols by well-managed grasslands but not annual grain or dairy forage cropping systems. *Proc. Natl. Acad. Sci. USA* **119**, e2118931119 (2022).
21. Angst, G. et al. Unlocking complex soil systems as carbon sinks: multi-pool management as the key. *Nat. Commun.* **14**, 2967 (2023).
22. Qin, S. et al. Temperature sensitivity of SOM decomposition governed by aggregate protection and microbial communities. *Sci. adv.* **5**, e1218 (2019).
23. Plante, A. F. et al. Decomposition temperature sensitivity of isolated soil organic matter fractions. *Soil. Biol. Biochem.* **42**, 1991–1996 (2010).
24. Karhu, K. et al. Similar temperature sensitivity of soil mineral-associated organic carbon regardless of age. *Soil. Biol. Biochem.* **136**, 107527 (2019).
25. Benbi, D. K., Boparai, A. K. & Brar, K. Decomposition of particulate organic matter is more sensitive to temperature than the mineral associated organic matter. *Soil. Biol. Biochem.* **70**, 183–192 (2014).
26. García-Palacios, P. et al. Dominance of particulate organic carbon in top mineral soils in cold regions. *Nat. Geosci.* **17**, 145–150 (2024).
27. Qin, S. et al. Linkage between temperature sensitivity of SOM decomposition and microbial communities depends on soil fractions. *Glob. Change Biol.* **30**, e17456 (2024).

28. Davidson, E. A. & Janssens, I. A. Temperature sensitivity of soil carbon decomposition and feedbacks to climate change. *Nature* **440**, 165–173 (2006).

29. Liáng, L. L., Kirschbaum, M. U., Arcus, V. L. & Schipper, L. A. The carbon-quality temperature hypothesis: Fact or artefact? *Glob. Change Biol.* **29**, 935–942 (2023).

30. Georgiou, K. et al. Emergent temperature sensitivity of soil organic carbon driven by mineral associations. *Nat. Geosci.* **17**, 205–212 (2024).

31. Gentsch, N. et al. Temperature response of permafrost soil carbon is attenuated by mineral protection. *Glob. Change Biol.* **24**, 3401–3415 (2018).

32. Yang, Z., Wullschleger, S. D., Liang, L., Graham, D. E. & Gu, B. Effects of warming on the degradation and production of low-molecular-weight labile organic carbon in an Arctic tundra soil. *Soil. Biol. Biochem.* **95**, 202–211 (2016).

33. Zhang, Q. et al. Whole-soil-profile warming does not change microbial carbon use efficiency in surface and deep soils. *Proc. Natl Acad. Sci. USA* **120**, e2302190120 (2023).

34. Girkin, N., Turner, B., Ostle, N. & Sjögersten, S. Composition and concentration of root exudate analogues regulate greenhouse gas fluxes from tropical peat. *Soil. Biol. Biochem.* **127**, 280–285 (2018).

35. Ye, C. et al. Reconciling multiple impacts of nitrogen enrichment on soil carbon: plant, microbial and geochemical controls. *Ecol. Lett.* **21**, 1162–1173 (2018).

36. Li, Y. et al. Oxygen availability regulates the quality of soil dissolved organic matter by mediating microbial metabolism and iron oxidation. *Glob. Chang. Biol.* **28**, 7410–7427 (2022).

37. Liu, F. et al. Divergent changes in particulate and mineral-associated organic carbon upon permafrost thaw. *Nat. Commun.* **13**, 5073 (2022).

38. Bååth, E. Temperature sensitivity of soil microbial activity modeled by the square root equation as a unifying model to differentiate between direct temperature effects and microbial community adaptation. *Glob. Chang. Biol.* **24**, 2850–2861 (2018).

39. Cox, P. M., Betts, R. A., Jones, C. D., Spall, S. A. & Totterdell, I. J. Acceleration of global warming due to carbon-cycle feedbacks in a coupled climate model. *Nature* **408**, 184–187 (2000).

40. Xu, X., Luo, Y. & Zhou, J. Carbon quality and the temperature sensitivity of soil organic carbon decomposition in a tallgrass prairie. *Soil. Biol. Biochem.* **50**, 142–148 (2012).

41. Qin, S. et al. Temperature sensitivity of permafrost carbon release mediated by mineral and microbial properties. *Sci. Adv.* **7**, eabe3596 (2021).

42. Hemingway, J. D. et al. Mineral protection regulates long-term global preservation of natural organic carbon. *Nature* **570**, 228–231 (2019).

43. Chen, C., Hall, S. J., Coward, E. & Thompson, A. Iron-mediated organic matter decomposition in humid soils can counteract protection. *Nat. Commun.* **11**, 2255 (2020).

44. Spaccini, R., Piccolo, A., Conte, P., Haberhauer, G. & Gerzabek, M. Increased soil organic carbon sequestration through hydrophobic protection by humic substances. *Soil. Biol. Biochem.* **34**, 1839–1851 (2002).

45. Kleber, M. et al. Dynamic interactions at the mineral–organic matter interface. *Nat. Rev. Earth Env.* **2**, 402–421 (2021).

46. Gillabel, J., Cebrian-Lopez, B., Six, J. & Merckx, R. Experimental evidence for the attenuating effect of SOM protection on temperature sensitivity of SOM decomposition. *Glob. Change Biol.* **16**, 2789–2798 (2010).

47. Moinet, G. Y. K. et al. The temperature sensitivity of soil organic matter decomposition is constrained by microbial access to substrates. *Soil. Biol. Biochem.* **116**, 333–339 (2018).

48. Hassink, J. The capacity of soils to preserve organic C and N by their association with clay and silt particles. *Plant. Soil.* **191**, 77–87 (1997).

49. Six, J., Conant, R. T., Paul, E. A. & Paustian, K. Stabilization mechanisms of soil organic matter: Implications for C-saturation of soils. *Plant. Soil.* **241**, 155–176 (2002).

50. Duan, P., Wang, K. & Li, D. Nitrogen addition effects on soil mineral-associated carbon differ between the valley and slope in a sub-tropical karst forest. *Geoderma* **430**, 116357 (2023).

51. Díaz-Martínez, P. et al. Vulnerability of mineral-associated soil organic carbon to climate across global drylands. *Nat. Clim. Chang.* **14**, 976–982 (2024).

52. Georgiou, K. et al. Global stocks and capacity of mineral-associated soil organic carbon. *Nat. Commun.* **13**, 3797 (2022).

53. Dettmann, U., Frank, S., Wittnebel, M., Piayda, A. & Tiemeyer, B. How to take volume-based peat samples down to mineral soil? *Geoderma* **427**, 116132 (2022).

54. Zhang, Z. et al. Urban development enhances soil organic carbon storage through increasing urban vegetation. *J. Environ. Manag.* **312**, 114922 (2022).

55. Penland, M. et al. Deciphering microbial community dynamics and biochemical changes during nyons black olive natural fermentations. *Front. Microbiol.* **11**, 586614 (2020).

56. Ma, T. et al. Divergent accumulation of microbial necromass and plant lignin components in grassland soils. *Nat. Commun.* **9**, 3480 (2018).

57. Liang, C., Amelung, W., Lehmann, J. & Kästner, M. Quantitative assessment of microbial necromass contribution to soil organic matter. *Glob. Chang. Biol.* **25**, 3578–3590 (2019).

58. Fang, C., Smith, P., Moncrieff, J. B. & Smith, J. U. Similar response of labile and resistant soil organic matter pools to changes in temperature. *Nature* **433**, 57–59 (2005).

59. Ding, J. et al. Linking temperature sensitivity of soil CO₂ release to substrate, environmental, and microbial properties across alpine ecosystems. *Glob. Biogeochem. Cy.* **30**, 1310–1323 (2016).

60. Bossio, D. A. & Scow, K. M. Impacts of carbon and flooding on soil microbial communities: phospholipid fatty acid profiles and substrate utilization patterns. *Microb. Ecol.* **35**, 265–278 (1998).

61. Bastida, F. et al. Soil microbial diversity–biomass relationships are driven by soil carbon content across global biomes. *ISME J.* **15**, 2081–2091 (2021).

62. Hu, J. et al. Photo-produced aromatic compounds stimulate microbial degradation of dissolved organic carbon in thermokarst lakes. *Nat. Commun.* **14**, 3681 (2023).

63. Xu, M. et al. High microbial diversity stabilizes the responses of soil organic carbon decomposition to warming in the subsoil on the Tibetan Plateau. *Glob. Chang. Biol.* **27**, 2061–2075 (2021).

64. Hu, A. et al. Ecological networks of dissolved organic matter and microorganisms under global change. *Nat. Commun.* **13**, 3600 (2022).

65. Bai, Y. et al. Long-term active restoration of extremely degraded alpine grassland accelerated turnover and increased stability of soil carbon. *Glob. Chang. Biol.* **26**, 7217–7228 (2020).

66. Fierer, N., Allen, A. S., Schimel, J. P. & Holden, P. A. Controls on microbial CO₂ production: a comparison of surface and subsurface soil horizons. *Glob. Chang. Biol.* **9**, 1322–1332 (2003).

67. Tang, X. et al. Carbon pools in China's terrestrial ecosystems: new estimates based on an intensive field survey. *Proc. Natl. Acad. Sci. USA* **115**, 4021–4026 (2018).

68. Chen, J. et al. A keystone microbial enzyme for nitrogen control of soil carbon storage. *Sci. Adv.* **4**, eaq1689 (2018).

Acknowledgements

This work was supported by National Natural Science Foundation of China (T2421005, T2261129474, 52039001, X.X.) and the National Key R&D Program of China (2017YFA0605001, X.X.).

Author contributions

X.X. and Z.Z. designed the study. Z.Z. and H.G. collected samples. Z.Z. and S.H. conducted the experiments. Z.Z., X.G., and E.L. performed data analysis. X.X., Z.Z., S.N., and E.L. wrote the manuscript. All authors contributed extensively to revising the paper.

Competing interests

The authors declare no competing interests.

Additional information

Supplementary information The online version contains supplementary material available at
<https://doi.org/10.1038/s41467-024-55765-y>.

Correspondence and requests for materials should be addressed to Xinghui Xia.

Peer review information *Nature Communications* thanks Olga Vindušková, Jinquan Li and Carmen Rosa Rosa Medina-Carmona for their contribution to the peer review of this work. A peer review file is available.

Reprints and permissions information is available at
<http://www.nature.com/reprints>

Publisher's note Springer Nature remains neutral with regard to jurisdictional claims in published maps and institutional affiliations.

Open Access This article is licensed under a Creative Commons Attribution-NonCommercial-NoDerivatives 4.0 International License, which permits any non-commercial use, sharing, distribution and reproduction in any medium or format, as long as you give appropriate credit to the original author(s) and the source, provide a link to the Creative Commons licence, and indicate if you modified the licensed material. You do not have permission under this licence to share adapted material derived from this article or parts of it. The images or other third party material in this article are included in the article's Creative Commons licence, unless indicated otherwise in a credit line to the material. If material is not included in the article's Creative Commons licence and your intended use is not permitted by statutory regulation or exceeds the permitted use, you will need to obtain permission directly from the copyright holder. To view a copy of this licence, visit <http://creativecommons.org/licenses/by-nc-nd/4.0/>.

© The Author(s) 2025